0022-3565/10/3331-129–139$20.00
THE JOURNAL OF PHARMACOLOGY AND EXPERIMENTAL THERAPEUTICS
JPET 333:129–139, 2010

Vol. 333, No. 1
163444/3569497
Printed in U.S.A.

Pharmacology and Antitumor Activity of ABC294640, a Selective Inhibitor of Sphingosine Kinase-2

Kevin J. French,[1] Yan Zhuang, Lynn W. Maines, Peng Gao, Wenxue Wang, Vladimir Beljanski, John J. Upson,[1] Cecelia L. Green, Staci N. Keller, and Charles D. Smith

Apogee Biotechnology Corporation, Hummelstown, Pennsylvania (K.J.F., Y.Z., L.W.M., J.J.U., C.L.G., S.N.K., C.D.S.); and Department of Pharmaceutical and Biomedical Sciences, Medical University of South Carolina, Charleston, South Carolina (P.G., W.W., V.B., C.D.S.)

Received November 6, 2009; accepted January 7, 2010

ABSTRACT

Sphingolipid-metabolizing enzymes control the dynamic balance of the cellular levels of important bioactive lipids, including the apoptotic compound ceramide and the proliferative compound sphingosine 1-phosphate (S1P). Many growth factors and inflammatory cytokines promote the cleavage of sphingomyelin and ceramide leading to rapid elevation of S1P levels through the action of sphingosine kinases (SK1 and SK2). SK1 and SK2 are overexpressed in a variety of human cancers, making these enzymes potential molecular targets for cancer therapy. We have identified an aryladamantane compound, termed ABC294640 [3-(4-chlorophenyl)-adamantane-1-carboxylic acid (pyridin-4-ylmethyl)amide], that selectively inhibits SK2 activity in vitro, acting as a competitive inhibitor with respect to sphingosine with a K_i of 9.8 μM, and attenuates S1P formation in intact cells. In tissue culture, ABC294640 suppresses the proliferation of a broad panel of tumor cell lines, and inhibits tumor cell migration concomitant with loss of microfilaments. In vivo, ABC294640 has excellent oral bioavailability, and demonstrates a plasma clearance half-time of 4.5 h in mice. Acute and chronic toxicology studies indicate that ABC294640 induces a transient minor decrease in the hematocrit of rats and mice; however, this normalizes by 28 days of treatment. No other changes in hematology parameters, or gross or microscopic tissue pathology, result from treatment with ABC294640. Oral administration of ABC294640 to mice bearing mammary adenocarcinoma xenografts results in dose-dependent antitumor activity associated with depletion of S1P levels in the tumors and progressive tumor cell apoptosis. Therefore, this newly developed SK2 inhibitor provides an orally available drug candidate for the treatment of cancer and other diseases.

Sphingolipids have become a focal point in biological research, with excellent rationale for their manipulation for the treatment of diseases, including cancer (reviewed in Ogretmen, 2006; Cuvillier, 2007; and Huwiler and Zangemeister-Wittke, 2007). The parent lipid sphingomyelin is a structural component of cellular membranes, but also serves as the precursor for potent second messengers that have profound cellular effects. Stimulus-induced metabolism of these lipids is critically involved in cancer cell biology and inflammatory diseases; hence, this metabolic pathway offers exciting new molecular targets for drug development.

In response to stimuli, including growth factors and inflammatory cytokines, sphingomyelin is enzymatically hydrolyzed to ceramide, which can be further hydrolyzed by the action of ceramidase to produce sphingosine. Ceramide and sphingosine induce apoptosis in cancer cells by mechanisms that remain to be elucidated. Sphingosine is rapidly phosphorylated by sphingosine kinase (SK) to produce sphingosine 1-phosphate (S1P), which is mitogenic and antiapoptotic. Through these conversions, a critical balance, i.e., a ceramide/S1P rheostat, has been hypothesized to determine the fate of the cell (Cuvillier et al., 1996). In this model, the balance between the cellular concentrations of ceramide and S1P determines whether a cell proliferates or undergoes apop-

This work was supported by the National Institutes of Health National Cancer Institute [Grants R43-CA097833, R01-CA122226].

[1] Current affiliation: GlaxoSmithKline, King of Prussia, Pennsylvania.

Article, publication date, and citation information can be found at http://jpet.aspetjournals.org.
doi:10.1124/jpet.109.163444.

ABBREVIATIONS: SK, sphingosine kinase; SK1, sphingosine kinase-1; SK2, sphingosine kinase-2; ABC294640, 3-(4-chlorophenyl)-adamantane-1-carboxylic acid (pyridin-4-ylmethyl)amide; DMS, *N*,*N*-dimethylsphingosine; NBD-Sph, omega(7-nitro-2–1,3-benzoxadiazol-4-yl)(2*S*,3*R*,4*E*)-2-aminooctadec-4-ene-1,3-diol; PBS, phosphate-buffered saline; PEG, polyethylene glycol; S1P, sphingosine 1-phosphate; FITC, fluorescein isothiocyanate; HPLC, high-performance liquid chromatography; LC/MS, liquid chromatography/mass spectrometry; TUNEL, terminal deoxynucleotidyl transferase dUTP nick-end labeling.

tosis. Upon exposure to mitogens or activation of intracellular oncoproteins, the cells experience an increase in the intracellular levels of S1P and depletion of ceramide levels, and this situation promotes cell survival and proliferation. In contrast, activation of sphingomyelinase in the absence of activation of ceramidase and/or SK results in the accumulation of ceramide and subsequent apoptosis.

Despite the high level of interest in sphingolipid-mediated signaling, there are very few known inhibitors of the enzymes of this pathway. In particular, the field suffers from a lack of potent and selective inhibitors of SK. Most pharmacological studies to date have used three compounds to inhibit SK activity: *N*,*N*-dimethylsphingosine (DMS), DL-*threo*-dihydrosphingosine, and *N*,*N*,*N*-trimethylsphingosine. However, these compounds are not specific inhibitors of SK because they have been shown to affect protein kinase C (Igarashi et al., 1989), 3-phosphoinositide-dependent kinase (King et al., 2000), and casein kinase II (McDonald et al., 1991). In addition, the compound phenoxodiol has been described as an SK inhibitor (Gamble et al., 2006); however, this isoflavone also inhibits several other enzymes. A few natural product inhibitors of SK have been isolated (Kono et al., 2001), but their selectivities remain unknown and their amenability to large-scale production is doubtful.

Inhibitors of SK that can be easily synthesized would clearly be highly desirable for evaluating this enzyme as a therapeutic target. To address this problem, we previously identified and characterized structurally novel inhibitors of SK (French et al., 2003, 2006). These compounds, called SKI-I, SKI-II, and SKI-V, inhibited S1P formation in intact cells, induced apoptosis, and demonstrated antitumor activity upon intraperitoneal administration (French et al., 2006), reinforcing the approach of targeting SK in cancer. We report here the pharmacological characterization of a new orally available SK inhibitor with in vivo activity. It is noteworthy that this compound is selective for SK2, thereby providing the first pharmacological probe to evaluate the biological roles of this SK isozyme.

Materials and Methods

Materials. Unless otherwise noted, all chemicals and reagents were purchased from Sigma-Aldrich (St. Louis, MO). Phalloidin-FITC were purchased from Invitrogen (Carlsbad, CA). Fibronectin and cell culture inserts were purchased from BD Biosciences (San Jose, CA). Recombinant human SK1 and SK2 were purchased from BPS Biosciences (San Diego, CA). C_{17}-sphingosine and C_{17}-S1P were purchased from Avanti Polar Lipids, Inc. (Alabaster, AL). All cell lines were obtained from the American Type Culture Collection and grown in either Dulbecco's modified Eagle's medium or RPMI 1640 medium containing 10% fetal bovine serum and 50 μg/ml gentamycin sulfate. ABC294640 (Fig. 1) was synthesized as described previously (Maines et al., 2008). The hydrochloride salt, ABC294640 · HCl, was prepared by dissolving 9.6 g of ABC294640 in 50 ml of CH_2Cl_2, and slowly adding an equimolar amount of 1M HCl in ether. After filtration and washing, 9.6 g (93%) of ABC294640 · HCl was recovered as fine crystals with a melting point of 204 to 206°C.

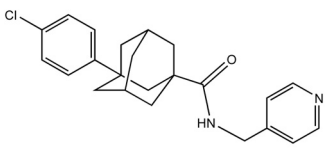

ABC294640

Fig. 1. Structure of ABC294640 (CAS 915385-81-8).

Sphingosine Kinase Assays. The IC_{50} values (the concentration that inhibits by 50%) for ABC294640 and DMS were determined by a newly developed HPLC-based SK activity assay. In brief, the test compounds were incubated with recombinant SK1 or SK2 and NBD-Sph in the isozyme-selective assay buffers detailed below with 1 mg/ml fatty acid-free bovine serum albumin, 100 μM ATP, and 400 μM $MgCl_2$. The product, i.e., NBD-S1P, was separated from NBD-Sph by HPLC as follows: Waters 2795 HPLC system with a Waters 2495 fluorescence detector, C8 Chromolith RP-8e column (100 × 4.6 mm; Merck KGaA, Darmstadt, Germany), 1 ml/min mobile phase (acetonitrile/20 mM sodium phosphate buffer, pH2.5, at 45:55). Fluorescence was monitored with excitation at 465 nm and emission at 531 nm. The ratio of NBD-S1P/(NBD-Sph + NBD-S1P) was used as a measure of SK activity. SK-isozyme selective assay buffers each contained 20 mM Tris, pH7.4, 5 mM EDTA, 5 mM EGTA, 3 mM β-mercaptoethanol, 5% glycerol, 1× protease inhibitors (Sigma-Aldrich) and 1× phosphatase inhibitors (Roche Diagnostics, Indianapolis, IN). For the SK1 assay buffer, 0.25% (final) Triton X-100 was added; and for the SK2 buffer, 1 M (final) KCl was added. Assays were run for 2 h at room temperature, and then a 1.5 volume of methanol was added to terminate the kinase reaction. After 10 min, the samples were centrifuged at 20,000*g* to pellet the precipitated protein, and the supernatants were analyzed by HPLC. In experiments to determine the K_i for inhibition of SK2 by ABC294640, the ADP Quest assay system (DiscoveRx Corporation, Fremont CA) was used to measure kinase activity in the presence of varying concentrations of sphingosine and ABC294640.

To determine the effects of ABC294640 on cellular SK activity, near-confluent MDA-MB-231 cells were serum-starved overnight, and then treated with varying concentrations of ABC294640. The cells were then incubated with [^{3}H]sphingosine at a final concentration of 1 μM as described previously (French et al., 2006). The cells take up the exogenous sphingosine, which is converted to S1P via SK activity, and [^{3}H]S1P is separated from [^{3}H]sphingosine by extraction and quantified by scintillation counting.

Sphingolipid Analyses. Biochemical analyses of ceramide species, sphingoid bases, and their phosphates were performed by the Lipidomics Shared Resource at the Medical University of South Carolina on a Thermo Finnigan TSQ 7000 triple-stage quadruple mass spectrometer (Thermo Fisher Scientific, Waltham, MA) operating in a Multiple Reaction Monitoring positive ionization mode. Quantitative analyses of the cellular sphingolipids were based on the calibration curves generated by spiking an artificial matrix with known amounts of target standards and an equal amount of the internal standard. The target analyte to internal standard peak area ratios from the samples were similarly normalized to their respective internal standards and compared with the calibration curves by linear regression. Final results were expressed as the level of the particular sphingolipid normalized the total phospholipid phosphate levels determined from the Bligh and Dyer lipid extract (Bielawski et al., 2006).

Cytotoxicity Assays. To determine the effects of the test compounds on proliferation, cells were plated into 96-well microtiter plates and allowed to attach for 24 h. Varying concentrations of ABC294640 were added to individual wells and the cells were incubated for an additional 72 h. At the end of this period, the number of viable cells was determined by use of the sulforhodamine-binding assay. The percentage of cells killed was calculated as the percentage decrease in sulforhodamine-binding compared with control cultures. Regression analyses of inhibition curves were performed by use of GraphPad Prism (GraphPad Software Inc., San Diego, CA).

Chemotaxis and Cytoskeletal Assays. Chemotaxis assays were performed as follows. Transwell inserts (8-μm pore size) were precoated with fibronectin (5 μg/ml) for 1 h at room temperature. A-498 cells were trypsinized and resuspended in serum-free media at

a concentration of 10^5 cells/ml. A total volume of 500 μl of this cell suspension was added to the top of the insert, and medium containing 10% fetal bovine serum was placed at the bottom to act as a chemoattractant. Equal concentrations of ABC294640 were added to the top and the bottom of the chamber. After 4 h at 37°C, cells that migrated through the membrane were fixed in 4% formaldehyde and stained with crystal violet. The number of migrating cells was established by counting ten random microscope fields. Experiments were performed in duplicate and repeated three times.

Microfilaments were stained with FITC-conjugated phalloidin (Invitrogen), according to the manufacturer's directions. In brief, cells in chamber slides were exposed to the vehicle, ABC294640 or cytochalasin B for various times, fixed in 3.7% paraformaldehide, permeabilized with 0.1% Triton X-100, blocked with 2% bovine serum albumin in Tris-buffered saline/Tween 20, and stained with 20 μl of phalloidin methanol solution per ml of blocking solution. After 12 to 16 h at 4°C, the excess phalloidin was removed by washing in Tris-buffered saline/Tween 20; cells were mounted and observed with a Zeiss LSM 510 laser scanning confocal microscope (Carl Zeiss GmbH, Jena, Germany). Cells were randomly selected, and at least five different images with multiple cells were taken per experimental point.

The G (globular) to F (fibrous) actin ratio was quantified to assess the status of microfilaments. In brief, cells were exposed to the drug for various times, and actin was extracted by washing the cells with 1% Triton X-100 solution in PBS. The two forms of actin were separated by centrifugation at 14,000*g*. The supernatant (containing G actin) was mixed 1:1 with Laemmli buffer, and the pellet (containing F actin) was dissolved in Laemmli buffer. Samples were subjected to SDS-polyacrylamide gel electrophoresis and the actin content of each fraction was quantified by immunoblotting with antiactin antibody and analyses using the ImageJ (National Institutes of Health) program.

Quantification of ABC294640 in Plasma and Tumors. Plasma samples were prepared by centrifugation (5000*g*, 5 min at 4°C) of whole blood that was collected into syringes containing EDTA as an anticoagulant. Samples were spiked with 10 μg of an internal standard {3-(4-chlorophenyl)adamantane-1-carboxylic acid [2-(3,4-dihydroxyphenyl)ethyl]amide}, brought to 1 ml with water and extracted three times with 2 ml of ethyl acetate. Extracts were dried over nitrogen at 35°C, reconstituted in 0.2 ml of 0.1% formic acid in water/methanol (50:50, phase A), filtered, and transferred to vials. Analyses were performed by use of an Agilent 1100 binary pump HPLC system coupled to a Finnigan LCQ Classic ion trap quadrupole mass spectrometer running in electrospray ionization positive ion mode. Sample (10 μl) was injected and resolved by use of a Supelco Discovery C18 column (2.1 × 20 mm, 5-mm particle size) connected to a Zorbax precolumn (Agilent Technologies, Santa Clara, CA) with a mobile phase consisting of 0.1% formic acid in water/methanol (50:50). The flow rate was 0.3 ml/min, and samples were eluted by a linear gradient increasing from 50 to 100% methanol over 3 min. ABC294640 and the internal standard were detected at 5.1 min and 5.5 min, respectively, by use of a selected ion monitoring mode (m/z = 381 and 426, respectively). Peak areas were integrated by use of Xcalibur software, and ABC294640 concentrations were determined from a standard curve, which was linear in range of all plasma levels observed in these studies.

Oral Bioavailability and Pharmacokinetic Studies. Formulations of ABC294640·HCl were administered orally or intravenously to fasted female Swiss-Webster mice at a dose of 100 mg/kg in 0.1 ml of the indicated solvents. Blood samples were removed at 1 and 7 h after dosing, and the plasma concentration of ABC294640 was determined by reverse-phase LC/MS running in SIM mode as described above. For pharmacokinetic studies, female Swiss-Webster mice (6–8 weeks old) were fasted overnight and administered a bolus dose of 0.1 ml of ABC294640 · HCl either orally or intravenously. After dosing, mice were anesthetized with halothane, and blood was removed via intracardiac puncture at the indicated times. Plasma samples were processed, and ABC294640 levels were determined as described above. Noncompartmental pharmacokinetic analyses were performed with use of WinNolin software package (Pharsight, Mountain View, CA).

Toxicology Studies. Acute (7-day) and chronic (28-day) toxicology studies were conducted with ABC294640·HCl. In the first study (which was conducted by Eurofins Product Safety Laboratories, Dayton, NJ), Sprague-Dawley male rats (7–8 weeks old) were orally dosed with 0, 100, or 250 mg of ABC294640·HCl/kg in 0.375% Polysorbate-80 in PBS daily for 7 days. The animals were observed daily for viability, signs of gross toxicity, and behavioral changes, and a battery of detailed observations were performed on study days 1 and 7. Blood was sampled from all animals on day 8 of the study for hematology, clinical biochemistry, and serology assessments, and the animals were sacrificed. Gross necropsies were performed on all study rats, and selected organs and tissues were evaluated in the control and high-dose level groups. In the second study, C57BL/6 mice were orally dosed with 0, 100, or 250 mg of ABC294640·HCl/kg daily exactly as indicated above, and sacrificed at either day 7 or day 28 for hematology studies.

Antitumor Evaluation. A syngeneic mouse tumor model that uses a transformed murine mammary adenocarcinoma cell line (JC, American Type Culture Collection number CRL-2116) and BALB/c mice (Charles River, Wilmington, MA) was performed as described previously (Lee et al., 2003). Animal care and procedures were in accordance with guidelines and regulations of the Institutional Animal Care and Use Committee of the Penn State College of Medicine. Animals were housed under 12-h light/dark cycles, with food and water provided ad libitum. Tumor cells (1×10^6) were implanted subcutaneously, and tumor volume was calculated by use of the equation: $(L \times W^2)/2$. On detection of tumors, mice were randomly assigned to treatment groups. Treatment was then administered every other day thereafter, consisting of oral doses of 3.5, 10, 35, or 100 mg of ABC294640·HCl/kg body weight or vehicle (0.375% Polysorbate-80). Whole body weights and tumor volume measurements were performed each day of treatment. On day 15, mice were dosed and euthanized 1 h later; tumors were excised and immediately frozen. p values were determined by use of one-way analysis of variance using GraphPad InStat.

Pharmacodynamic Studies and Tumor Accumulation of ABC294640. Apoptosis was measured in sections from tumors treated with ABC294640·HCl using a TUNEL detection kit according to the manufacturer's instructions (In situ cell death detection kit; Roche Diagnostics). In brief, tumor sections were incubated with permeabilization solution (0.1% Triton X-100, 0.1% sodium citrate, freshly prepared) for 8 min at room temperature and then washed twice with PBS. Sections were incubated with TUNEL reaction mixture in a humid atmosphere at 37°C for 60 min and mounted with crystal mounting medium. The amount of apoptosis was calculated for an average of 10 microscopic fields in each sample (magnification, 100×) and expressed as the percentage of cells that were TUNEL-positive. For the analyses of sphingolipids, frozen tumor slices were homogenized in ice-cold PBS to a final concentration of 10 mg/ml. A 0.5-ml aliquot of the homogenate was combined with 0.5 ml of methanol, 0.25 ml of chloroform, and 375 pmol each of internal standards C_{17}-sphingosine and C_{17}-S1P. Blank samples spiked with known amounts of sphingosine, S1P, and the internal standards were processed in parallel to provide a standard curve for quantification. After sonication, samples were incubated overnight at 48°C, followed by addition of 75 μl of 1 N potassium hydroxide in methanol. The samples were then sonicated and incubated at 37°C for 2 h. A portion (0.4 ml) of each sample was then transferred to a new tube, dried, reconstituted in 0.25 ml of phase A, filtered, and transferred to a vial. HPLC was performed as described above. Elution was performed at 0.45 ml/min with 65% phase B for 2 min followed by a linear gradient to 100% phase B over 5 min. Ions for C_{17}-sphingosine, sphingosine, C_{17}-S1P, and S1P were monitored at m/z 286 (parent ion) → 268 (daughter ion), 300 → 282, 366 → 250, and 380 → 264, respectively.

Likewise, extracts of tumors from ABC294640-treated mice were prepared and levels of ABC294640 were quantified by LC/MS as described above.

Results

Inhibition of Sphingosine Kinase Activity by ABC294640. Screening of a chemical library identified SK inhibitors containing an aryladamantane scaffold, and approximately 140 congeners were synthesized and tested for their ability to inhibit a recombinant fusion protein of glutathione *S*-transferase and human SK1 (Smith et al., 2008). The structure-activity properties of this series will be reported elsewhere. Although ABC294640 is not the most potent SK inhibitor in this series, its biological and pharmacological properties were characterized because of its excellent solubility and oral absorption (described below), and in vivo activity in models of diabetic retinopathy (Maines et al., 2006) and ulcerative colitis (Maines et al., 2008).

In evaluating the potencies of these compounds, we developed an HPLC-based assay for SK activity that avoids the use of radiolabeled substrate as we have described previously (French et al., 2003). Using recombinant human SK1 and SK2, ABC294640 demonstrated dose-dependent inhibition of SK2 with an IC_{50} of approximately 60 μM without affecting the activity of SK1 at concentrations up to at least 100 μM (Fig. 2A). In contrast, DMS inhibited both SK1 and SK2 with IC_{50} values of approximately 60 and 20 μM, respectively. Additional studies demonstrated that both ABC294640 and DMS act as competitive inhibitors with respect to sphingosine, making the IC_{50} strongly affected by the concentration of sphingosine used in the assay. Kinetic analyses of varying concentrations of ABC294640 in the presence of 2.5 to 25 μM sphingosine indicated a K_i of 9.8 ± 1.4 μM for the inhibition of SK2 (Fig. 2B).

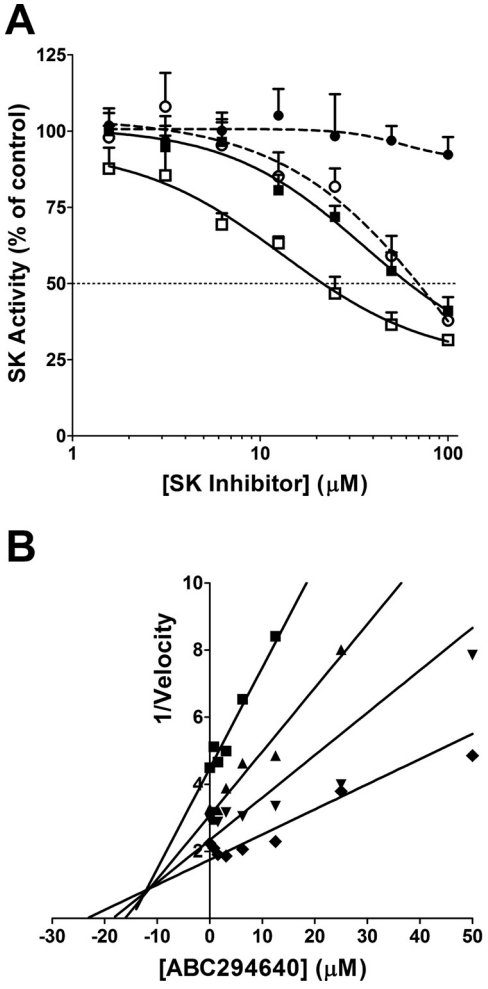

Fig. 2. Inhibition of sphingosine kinases. A, recombinant SK1 (circles) or SK2 (squares) was incubated with the indicated concentrations of ABC294640 (●, ■) or DMS (○, □), and the kinase activity was measured by use of the HPLC assay described under *Materials and Methods*. Values represent the mean ± S.E.M. for three experiments. B, recombinant SK2 was incubated with the indicated concentration of ABC294640, and kinase activity was determined in assays containing 2.5 (■), 5 (▲), 10 (▼), or 25 (♦) μM sphingosine by use of the ADP Quest assay as described under *Materials and Methods*. The reciprocal of the velocity is plotted against the ABC294640 concentration providing a Dixon plot of the results.

To assess its selectivity, ABC294640 was tested against a panel of serine/threonine and tyrosine protein kinases, several of which are regulated by interactions with lipids. Each kinase was incubated with its appropriate peptide substrate, ATP, and 50 μM ABC294640. Activities were normalized to vehicle-treated (dimethyl sulfoxide) control reactions. As indicated in Table 1, none of the other 20 diverse kinases tested were significantly inhibited by the compound. These data suggest that the biological effects of this compound are not mediated by off-target inhibition of protein kinases, consistent with its targeting of the sphingosine binding site of SK2.

It was also important to determine the ability of ABC294640 to inhibit endogenous SK activity in an intact cell model. Therefore, we used our previously described method in which MDA-MB-231 cells are incubated with [^{3}H]sphingosine at a final concentration of 1 μM (French et al., 2003). The cells take up the exogenous sphingosine, which is converted to S1P via SK activity, and the cells are harvested and [^{3}H]S1P is separated from [^{3}H]sphingosine by extraction and quantified by scintillation counting. In this assay, ABC294640 decreased [^{3}H]S1P formation in a dose-dependent fashion with an IC_{50} value of 26 μM. To confirm the affects of ABC294640 on endogenous SK activity, the time dependence of alteration of the sphingolipid profile in JC murine adenocarcinoma cells was assessed by lipidomic profiling. As demonstrated in Fig. 3, the predominant molecular species of ceramide in untreated cells included C_{16}-ceramide, C_{22}-ceramide, C_{24}-ceramide, and $C_{24:1}$-ceramide. Each of these molecular species of ceramide was elevated after 12 and 24 h of ABC294640

TABLE 1

Kinase selectivity of ABC294640

The effects of 50 μM ABC294640 on the activities of the indicated protein kinases was assessed by Upstate Cell Signaling. Values represent percentage of activity of the indicated kinase remaining in the presence of ABC294640 and are the mean ± S.D. of duplicate measurements.

Kinase	Activity	Kinase	Activity
	% control		*% control*
Ca^{2+}/calmodulin PK IV	81 ± 3	cRaf	96 ± 5
Abl	98 ± 0	MEK kinase 1	104 ± 3
Aurora-A	103 ± 1	CHK1	142 ± 13
Protein kinase C α	86 ± 5	EFGR	101 ± 3
Protein kinase C ε	101 ± 1	Fyn	84 ± 5
CDK1/cyclinB	105 ± 1	cSrc	115 ± 3
CDK2/cyclinE	106 ± 6	IKKα	150 ± 16
p38 MAP kinase 1	94 ± 2	PKA	104 ± 5
p38 MAP kinase 2	109 ± 5	PKBα	95 ± 2
PDK1	116 ± 3	PKBγ	105 ± 8

MEK, mitogen-activated protein kinase kinase; IKK, IκB kinase complex; MAP, mitogen-activated protein; PKA, protein kinase A.

treatment, but these changes were largely normalized by 48 h of treatment. It is noteworthy that the cellular levels of dihydro-C_{16}-ceramide were dramatically and persistently elevated by treatment with ABC294640, as were levels of dihydro-sphingosine. It is noteworthy that cellular S1P levels were decreased at all times of ABC294640 treatment, in particular, in cells treated for 48 h. Therefore, ABC294640 markedly alters the ratio of ceramide/S1P consistent with inhibition of SK activity.

Inhibition of Tumor Cell Proliferation and Migration by ABC294640. The effects of ABC294640 on the proliferation of human tumor cell lines representing major tumor types were determined by use of the sulforhodamine B assay for quantifying cell number. As indicated in Table 2, ABC294640 inhibited tumor cell proliferation with IC_{50} values ranging from approximately 6 to 48 μM with Hep-G2 and HT-29 cells being the most and least sensitive, respectively. It is notable that the IC_{50} for inhibition of the proliferation of MDA-MB-231 cells closely matches the IC_{50} for suppression of SK activity in this cell line, i.e., 29 and 26 μM, respectively, supporting the hypotheses that the antiproliferative effects of ABC294640 are mediated by inhibition of SK activity, and that SK2, in particular, is important for cell proliferation.

Binding of S1P to G protein-coupled S1P receptors induces a plethora of biological effects, including rapid reorganization of the actin cytoskeleton and stimulated migration of the cells (Hait et al., 2006). Therefore, we hypothesized that inhibition of SK activity by ABC294640 will affect microfilament structure and the ability of cells to migrate. A-498 cells are highly metastatic and mobile, which allowed us to perform migration assays by use of Boyden chambers for a short time (4 h). As shown in Fig. 4A, even short exposure to ABC294640 affected the ability of A-498 cells to migrate through a filter. This was confirmed using the "scratch assay," which measures haptokinetic (random) cell movement (data not shown). Because cell migration depends on the microfilament cytoskeleton, A-498 cells were treated with ABC294640 and actin fibers were stained with FITC-phalloidin and observed by confocal microscopy. Representative images from those experiments are presented in Fig. 4C in which actin fibers are stained green and nuclei are stained blue with 4,6-diamidino-2-phenylindole. Cytochalasin D was used as a positive control for microfilament depolymerization. At the 24-h time point and concentrations of 50 μM or higher, the most noticeable phenotypes were a decrease in the number of stress fibers in the cells and a decrease in the number of lamellipodia protruding from the cell surface. Reorganization of actin structure was confirmed by separating and measuring the globular (G) and fibrous (F) actin levels. As shown on Fig. 4B, the increase in G/F actin ratio is consistent with the changes in actin structure observed by confocal microscopy.

Absorption of ABC294640. The HCl salt of ABC294640 (ABC294640·HCl) has been synthesized in multigram amounts for characterizations of its toxicity, pharmacokinetics, and in vivo efficacy. Formulation analyses were conducted to identify a suitable pharmaceutical composition for in vivo studies. We chose five different oral formulations from the *Division of Drug Information Resources' Inactive Ingredient Guide*, a compen-

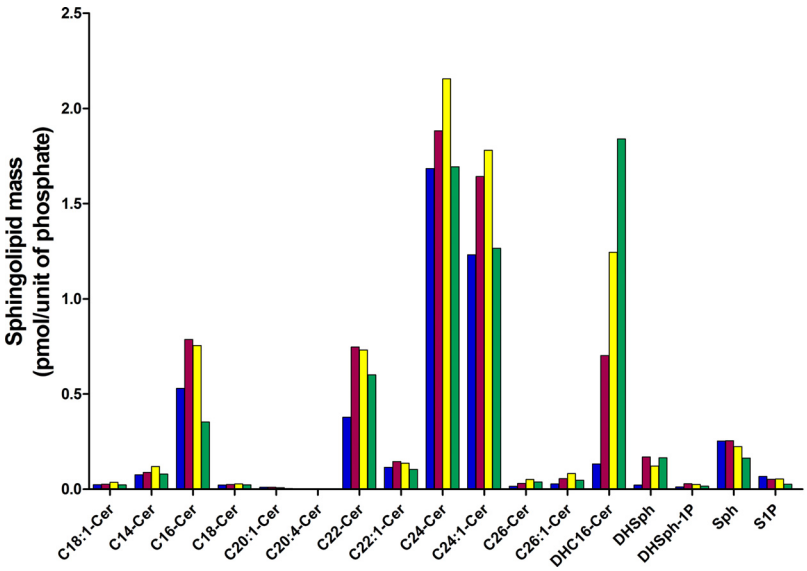

Fig. 3. Time course of sphingolipid alterations by ABC294640. JC murine adenocarcinoma cells were exposed to 40 μM ABC294640 for 0 (blue), 12 (red), 24 (yellow), or 48 (green) h. Cells were harvested and the masses of the indicated sphingolipid species were quantified by mass spectrometry in the Lipidomics Core Facility as described under *Materials and Methods*. Labels indicate the chain length and saturation of molecular species of ceramide (Cer). Other labels refer to dihydro-C_{16}-ceramide (DHC16-Cer), dihydrosphingosine (DHSph), dihydrosphingosine 1-phosphate (DhSph-1P), sphingosine (Sph), and S1P.

TABLE 2

Effects of ABC294640 on tumor cell proliferation

Sparsely plated cells were treated with ABC294640 for 48 h, and the number of viable cells was determined and compared with vehicle (DMSO)-treated cells as described in *Materials and Methods*. Values are the mean ± S.E.M. for at least three separate experiments.

Cell Line	Tissue	IC_{50}	Cell Line	Tissue	IC_{50}
		μM			μM
1025LU	Melanoma	33.7 ± 2.7	Hep-G2	Liver	6.0 ± 2.6
A-498	Kidney	12.2 ± 6.0	MCF-7	Breast, ER+	18.4 ± 7.4
Caco-2	Colon	11.8 ± 5.6	MDA-MB-231	Breast, ER−	29.1 ± 11.1
HT-29	Colon	48.1 ± 7.6	Panc-1	Pancreas	32.8 ± 0.1
DU145	Prostate	21.9 ± 1.5	T24	Bladder	39.4 ± 7.4
SK-OV-3	Ovary	10.5 ± 2.6			

ER+, estrogen receptor positive; ER−, estrogen receptor negative.

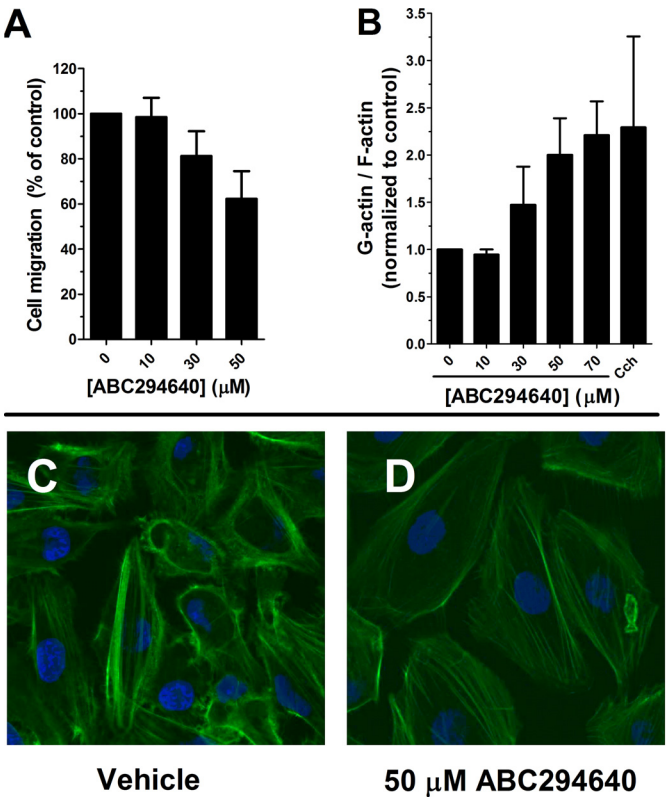

Fig. 4. Disruption of tumor cell migration and microfilament structure by ABC294640. A, A-498 cells were plated into a Boyden chamber and treated with the indicated concentration of ABC294640 for 4 h as described in *Materials and Methods*. The number of cells migrating to the opposite side of the filter was then quantified. B, A-498 cells were treated with the indicated concentration of ABC294640 for 24 h, and the amounts of G-actin and F-actin were determined as described in *Materials and Methods*. Cytochalasin D (cch) was used as a positive control at a concentration of 1 μM. C and D, A-498 cells were treated with 0 (C) or 50 μM ABC294640 (D) for 24 h, and then stress fibers were visualized with FITC-phalloidin as described under *Materials and Methods*.

dium of all inactive ingredients in approved drug products currently marketed for human use, to assess their ability to support oral absorption of ABC294640. Solutions of ABC294640·HCl in water, 90% propylene glycol, 100% polyethylene glycol 400 (PEG400), 50% PEG400 or 0.375% Polysorbate-80 did not precipitate (measured as turbidity at 590 nm), and so were administered to fasted female Swiss-Webster mice at a dose of 100 mg/kg. Blood samples were removed at 1 and 7 h, and plasma levels of ABC294640 were determined by use of an internal standard and reverse-phase HPLC coupled to an ion-trap quadrupole mass spectrometer running in positive SIM detection mode. As shown in Table 3, substantial amounts of ABC294640 were detected in the blood 1 h after oral dosing, with the highest levels attained in the samples formulated in 90% propylene glycol. It should be noted that these ABC294640 concentrations are sufficient to inhibit SK activity and proliferation of tumor cells. By 7 h, the plasma concentrations decreased by approximately 50% in most cases. Effective absorption was observed in the sample formulated in 0.375% Polysorbate-80, and this solvent for ABC294640·HCl was used in further pharmacokinetic and efficacy analyses because of its low toxicity.

TABLE 3

Effects of formulation on the oral absorption of ABC294640

Mice were dosed with 100 mg/kg ABC294640 dissolved in the indicated carriers, and plasma levels of the compound were determined at indicated times. Values represent the mean ± S.E.M. (n = 3 per group) concentration of plasma ABC294640.

Formulation	Plasma ABC294640	
	1 h	7 h
	μM	
Water	34.0 ± 4.7	8.2 ± 2.2
90% Propylene glycol	62.0 ± 11.8	23.5 ± 1.6
100% PEG400	48.9 ± 0.1	28.6 ± 8.6
50% PEG400	31.3 ± 0.5	29.3 ± 11.3
0.375% Polysorbate-80	51.6 ± 0.9	27.3 ± 9.8

To further understand the absorption properties of ABC294640·HCl, the relationship between plasma concentration and dose was examined. Mice were orally dosed with 10, 35, or 100 mg/kg ABC294640, and the plasma levels were determined at 30 min. As shown in Fig. 5, the plasma ABC294640 values demonstrated a good linear response with doses up to at least 100 mg/kg.

Pharmacokinetics of ABC294640. Detailed pharmacokinetic studies were performed on ABC294640·HCl in 0.375% Polysorbate-80. Female Swiss-Webster mice were dosed with 50 mg/kg ABC294640 either intravenously or orally. Groups of mice (3 per group) were anesthetized, and blood was removed via cardiac puncture at time points ranging from 1 min to 7 h. Plasma concentrations of ABC294640 were determined by LC/MS, and pharmacokinetic parameters were calculated by use of the WinNolin software package (Table 4). Intravenous administration of ABC294640 resulted in high plasma concentrations that were eliminated with a half-time of clearance of 1.4 h. Although the peak plasma level of ABC294640 was lower when the compound was administered by oral gavage, the compound was much more persistent, probably reflecting continued absorption from the gastrointestinal tract, such that the calculated half-time for clearance was 4.5 h. It is noteworthy that comparison of the oral versus the intravenous pharmacokinetics of ABC294640 indicated an excellent oral bioavailability of 66% ($F = AUC_{oral}/AUC_{iv}$).

Toxicity of ABC294640. Preliminary toxicity studies were performed to determine the appropriate dose for in vivo efficacy testing. No immediate or delayed toxicity was observed in female Swiss-Webster mice treated with intraperitoneal doses of ABC294640·HCl up to at least 250 mg/kg. Repeated injections in the same mice every other day over 15 days showed a similar lack of toxicity at doses up to at least 250 mg/kg. Dose-escalation toxicity testing was performed via oral gavage with ABC294640·HCl dissolved in 0.375% Polysorbate-80, and no toxic effects were observed after ad-

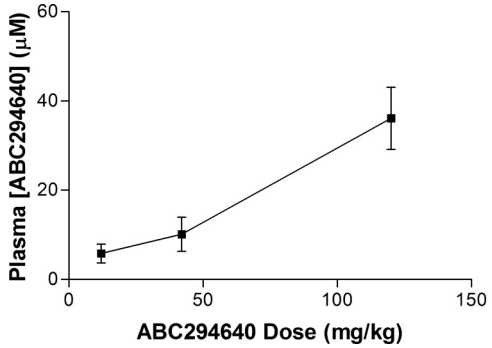

Fig. 5. Relationship between dose and plasma ABC294640 level. Mice were orally dosed with the indicated amounts of ABC294640·HCl in 0.375% Polysorbate-80 and bled at 30 min; the concentration of ABC294640 in the plasma was determined as described under *Materials and Methods*. Values represent mean ± S.E.M. (n = 3 mice per group).

TABLE 4

Pharmacokinetics of ABC294640

Mice were given 50 mg/kg ABC294640·HCl in 0.375% Polysorbate-80 intravenously or by oral gavage Plasma was harvested at times between 1 min and 7 h, and ABC294640 levels were determined as described in *Materials and Methods*. Values represent the mean ± S.E.M. ($n = 3$ per group).

Route	$AUC_{0\to\infty}$	$AUC_{0\to\infty}$	t_{max}	C_{max}	C_{max}	$t_{1/2}$
	$\mu g \cdot h/ml$	$\mu M \cdot h$	h	$\mu g/ml$	μM	h
Intravenous	56.9	137	0	31.1	74	1.4
Oral	37.5	90.1	0.25	8	19	4.5

AUC, area under the curve.

ministration of doses up to 1000 mg/kg. Therefore, the compound was considered to be suitable for more detailed in vivo studies.

Non-good laboratory practice acute toxicology studies were contracted to Eurofins|Product Safety Laboratories, in which ABC294640·HCl was given orally in 0.375% Polysorbate-80 to rats at doses of 0, 100, or 250 mg/kg daily for 7 days. There were no clinical observations or gross findings that were considered to be the result of ABC294640·HCl administration or otherwise. There were no significant changes in total body weight of the treated animals, although there was a slight decrease in body weight gain, consistent with a small decrease in food consumption, in the high-dose rats. Hematology studies (Table 5) indicated decreases in red blood cell number and hematocrit of approximately 20% in animals given either 100 or 250 mg/kg/day; and a slight increase in neutrophils and decrease in basophils in the treated rats. These changes would be scored as grade 0 toxicities on the standard National Cancer Institute scale for evaluating toxicity in clinical trials. It is noteworthy that no decreases in lymphocyte, platelet, or granulocyte counts were observed, indicating that the compound does not induce immunologic toxicities that are common with other anticancer drugs. Likewise, there were no drug-induced alterations of a broad panel of clinical chemistry or coagulation parameters. No gross abnormalities were noted for any of the euthanized animals when necropsied at the end of the 7-day observation period. Likewise, there were no treatment-related microscopic changes in any organ examined in the high-dose group, except for a slight decrease in the background level of extramedullary hematopoiesis in the spleen that may underlie the small decreases in the hematocrit.

To further characterize the hematologic changes observed in the acute study, mice were treated with 0, 100, or 250 mg of ABC294640·HCl/kg daily for 28 days. As indicated in Fig. 6A, mice treated with 250 mg/kg experienced a 20% decrease in red blood cell count and hematocrit, and a modest increase in the number of circulating neutrophils on day 7, essentially identical to the previous study with rats. However, after 28 days of treatment (Fig. 6B), these parameters were restored to normal levels, indicating that the animals had fully recovered from any transient impairment of hematopoiesis. In addition, there were no changes in the brain or spleen weights of treated mice, whereas a slight decrease (12%) in liver weight was observed in mice treated with 250 mg/kg.

Antitumor Activity of ABC294640. The antitumor activity of ABC294640·HCl was tested in a syngeneic tumor model that uses the mouse JC mammary adenocarcimona cell line growing subcutaneously in immunocompetent BALB/c mice (Lee et al., 2003). Because of the excellent oral absorption described above, we determined the ability of orally delivered ABC294640·HCl to reduce tumor growth in vivo. The SK inhibitor was administered to fasted mice on odd days at doses ranging from 3.5 to 100 mg/kg. Body weights and tumor volumes were monitored daily. As demonstrated in Fig. 7, ABC294640·HCl caused dose-dependent reductions in the growth of the mammary adenocarcinoma xenografts. Body weights in each treatment group remained unchanged from vehicle-treated mice during the course of the study (data not shown). Comparison with the potencies in the tumor studies with the toxicity data described above reveals that ABC294640·HCl has a therapeutic index of greater than 7 (250 mg/kg nontoxic dose / 35 mg/kg antitumor activity). Thus, this SK2 inhibitor has an excellent therapeutic index.

To ensure that the antitumor effect of ABC294640·HCl administration is mediated by the compound, its accumulation in tumors was quantified by LC/MS. In these experiments, mice bearing JC tumor xenografts were treated with 100 mg/kg ABC294640·HCl by intraperitoneal injection, and the concentrations of the compound in the plasma and the tumor were measured at 2 and 5 h. As indicated in Fig. 8A, approximately 75 μg/ml (197 μM) ABC294640 was present in the plasma at 2 h, and this decreased to 56 μg/ml (147 μM) at 5 h. The amounts of ABC294640 in the tumor at 2 and 5 h were determined to be 36 and 54 μg/g wet weight, respectively, corresponding to approximately 94 and 140 μM (assuming that 1 g approximately equals 1 ml). Therefore, amounts of ABC294640 well above those needed to block cell proliferation are accumulated in the tumors of intact mice.

TABLE 5

Summary of hematologic effects of ABC294640

Sprague-Dawley rats were treated with 0, 100, or 250 mg of ABC294640·HCl/kg for 7 days as described in *Materials and Methods*. Values represent the mean ± S.D. for 5 rats per group.

Parameter	Units	Dose		
		0	100	250
Erythrocyte count	$10^6/\mu l$	7.52 ± 0.23	6.00 ± 0.20[a]	5.92 ± 0.28[a]
Hematocrit	%	41.9 ± 0.8	33.8 ± 0.8[a]	32.7 ± 1.8[a]
Absolute reticulocyte count	$10^3/\mu l$	350 ± 59	431 ± 14[a]	355 ± 41
Platelet count	$10^3/\mu l$	734 ± 181	1201 ± 300[a]	950 ± 301
Total leukocyte count	$10^3/\mu l$	14.48 ± 0.80	12.74 ± 2.09	15.24 ± 3.23
Absolute neutrophils	$10^3/\mu l$	1.75 ± 0.43	2.09 ± 0.33	2.98 ± 0.50
Absolute lymphocytes	$10^3/\mu l$	11.99 ± 0.86	9.96 ± 1.67	11.69 ± 2.81
Absolute monocytes	$10^3/\mu l$	0.35 ± 0.12	0.39 ± 0.21	0.28 ± 0.08
Absolute eosinophils	$10^3/\mu l$	0.27 ± 0.14	0.17 ± 0.07	0.15 ± 0.04
Absolute basophils	$10^3/\mu l$	0.06 ± 0.01	0.04 ± 0.01[a]	0.05 ± 0.01[a]
Absolute large unstained cells	$10^3/\mu l$	0.07 ± 0.01	0.08 ± 0.02	0.08 ± 0.02

[a] Statistically significant difference from control at $p < .05$ by the Dunnett/Tamhane-Dunnett test.

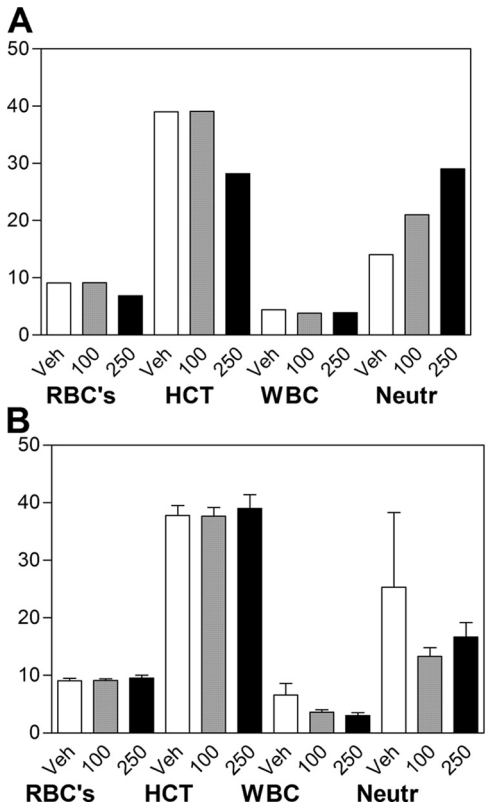

Fig. 6. Hematologic parameters in ABC294640-treated mice. Mice were orally dosed with 0 (Veh), 100 or 250 mg/kg ABC294640·HCl in 0.375% Polysorbate-80 daily for either 7 (A) or 28 (B) days. Blood was harvested by cardiac puncture and a complete blood count was performed. Values represent mean ± S.E.M. (n = 3 or 4 mice per group) for the red blood cells (RBC), hematocrit (HCT), total white blood cell (WBC), and neutrophil (Neutr) values.

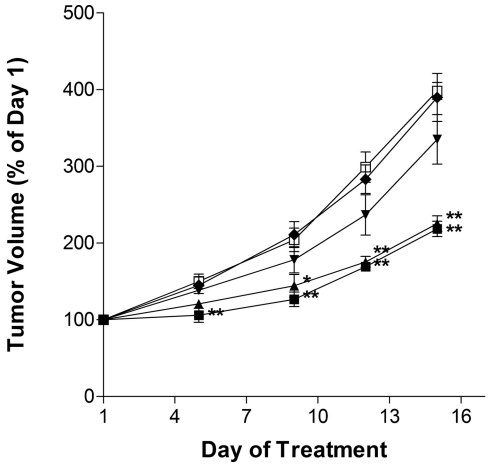

Fig. 7. Antitumor activity of orally administered ABC294640. Female BALB/c mice were injected subcutaneously with JC cells suspended in PBS. After palpable tumor growth, animals were treated every other day by oral gavage with 0 (□), 3.5 (♦), 10 (▼), 35 (▲), or 100 (■) mg/kg ABC294640·HCl in 0.375% Polysorbate-80. Values represent the mean ± S.E.M. (n = 5 mice per group) tumor volume normalized to treatment day 1 for each mouse. *, $p < 0.05$; **, $p < 0.01$.

As a global pharmacodynamic endpoint for ABC294640·HCl treatment, tumors from mice given a single dose of the compound were scored for their apoptotic indices by use of the TUNEL method. As shown in Fig. 8B, untreated tumors had focal areas of apoptosis such that the overall tumor apoptosis

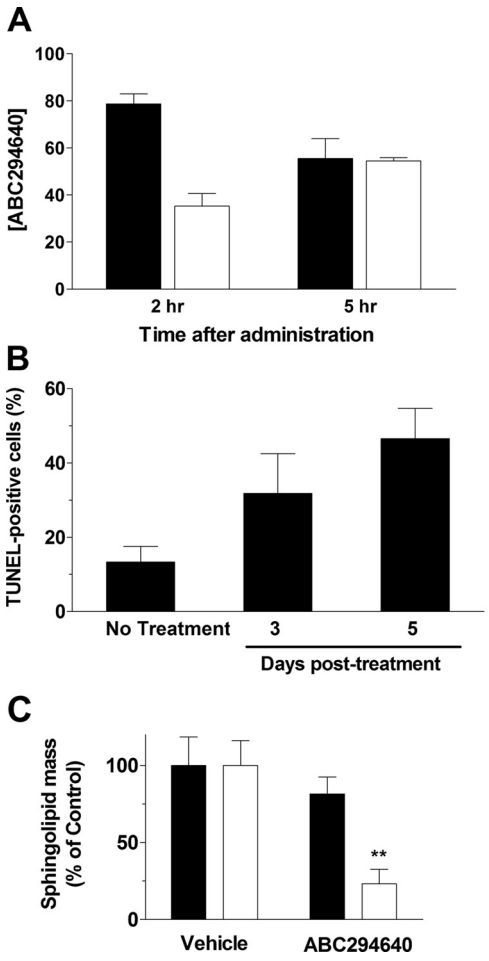

Fig. 8. Pharmacodynamic effects of ABC294640. A, accumulation of ABC294640 in tumors. Mice bearing JC tumor xenografts were treated by intraperitoneal injection of 100 mg/kg ABC294640·HCl, and tumors were harvested at the 2 or 5 h. The tumors were homogenized, and the amount of ABC294640 was quantified (n = 4 mice per group). Values represent the mean ± S.E.M. in micrograms per milliliter for plasma samples (filled bars) and micrograms per gram wet weight for tumor samples (open bars). B, induction of tumor apoptosis by ABC294640. Mice bearing JC tumor xenografts were treated by intraperitoneal injection of 100 mg/kg ABC294640·HCl. Tumors were harvested either 3 or 5 days after drug treatment, fixed, and sectioned, and the amount of apoptosis was quantified as TUNEL staining. Values represent the mean ± S.E.M. percentage of tumor cells that were TUNEL-positive (n = 4 mice per group). C, alteration of S1P levels by ABC294640. Tumors were harvested at the end of the experiment described in Fig. 7. The levels of sphingosine (filled bars) or S1P (open bars) were determined by liquid chromatography/tandem mass spectrometry. Values represent the mean ± S.D. levels compared with the vehicle-treatment group. **, $p < 0.01$ versus vehicle-treated mice.

index was approximately 12%. Treatment of the mice with 100 mg/kg ABC294640·HCl enhanced tumor cell apoptosis in a time-dependent manner, such that nearly 50% of the tumor cells expressed fragmented DNA by 5 days.

To determine a mechanistic pharmacodynamic endpoint for ABC294640·HCl, we quantified sphingolipid metabolites in the tumors by liquid chromatography/tandem mass spectrometry. Samples of frozen tumors removed at the end of the study in Fig. 7 were homogenized in cold PBS, spiked with internal standards, and processed by liquid-liquid extraction. Ratios of sphingosine and S1P to internal standards were determined and compared with vehicle-treated tumor samples. As shown in Fig. 8C, treatment of the mice with

ABC294640·HCl at the 100 mg/kg dose had no effect on sphingosine levels in the tumors. This lack of effect is probably due to the rapid conversion of sphingosine to ceramide in the presence of the SK inhibitor. It is noteworthy that S1P levels were significantly reduced in the tumors of mice treated with ABC294640·HCl. These findings provide further evidence that the antitumor activity of this compound is linked to SK inhibition and decreased S1P formation.

Discussion

Accumulating evidence demonstrates that S1P is a critical second messenger that exerts proliferative, antiapoptotic, and inflammatory actions. An oncogenic role of SK has been directly demonstrated, because transfection into NIH/3T3 fibroblasts was sufficient to promote foci formation and cell growth in soft agar, and to allow these cells to form tumors in nonobese diabetic/severe combined immunodeficiency mice (Xia et al., 2000). In addition, inhibition of SK by transfection with a dominant-negative SK mutant or by treatment of cells with the nonspecific SK inhibitor DMS blocked transformation mediated by oncogenic H-Ras. Because abnormal activation of Ras frequently occurs in cancer, these findings suggest a significant role of SK in this disease. SK has also been linked to estrogen signaling (Sukocheva et al., 2003) and estrogen-dependent tumorigenesis in MCF-7 cells (Nava et al., 2002). Other pathways or targets to which SK activity has been linked in cancer include vascular endothelial growth factor signaling via the Ras and mitogen-activated protein kinase pathway (Shu et al., 2002), protein kinase C (Nakade et al., 2003), tumor necrosis factor α (Vann et al., 2002), and caspase activation (Edsall et al., 2001). Angiogenic factors and processes, such as cell motility, mitogenesis in smooth muscle cells, endothelial cell differentiation, and growth factor signaling are also affected by SK and S1P (Lee et al., 1999). Although the elucidation of downstream targets of S1P remains an interesting problem in cell biology, sufficient validation of these pathways has been established to justify their evaluation as targets for new types of anticancer drugs. Because S1P seems to be the most direct mitogenic messenger, inhibition of its production should have useful antiproliferative effects on tumor cells.

Two isozymes of SK (termed SK1 and SK2) exist (Kohama et al., 1998); SK2 was cloned in 2000 (Liu et al., 2000). However, the roles of these SK isozymes remain to be defined because they demonstrate different kinetic parameters and expression patterns in normal tissue. The majority of studies linking SK activity to cancer and growth control have focused on SK1 (Nava et al., 2002; Johnson et al., 2005; Le Scolan et al., 2005; Pchejetski et al., 2005; Sarkar et al., 2005; Kawamori et al., 2006). For example, epidermal growth factor rapidly induces the expression of SK1, but not SK2, in MCF-7 cells (Döll et al., 2005); however, it has also been reported that epidermal growth factor activates SK2 in MDA-MB-453 cells (Hait et al., 2005). Overexpression of SK1 has been shown to be oncogenic in a variety of cells (Xia et al., 2000; French et al., 2003; Le Scolan et al., 2005), whereas overexpression of SK2 is reported to inhibit cell growth and to induce apoptosis (Maceyka et al., 2005). However, these effects of SK2 only partially depend on its catalytic activity, suggesting that the antiproliferative effects may be mediated by its BH3 domain (Maceyka et al., 2005). Consistent with this finding, are the observations that physiological levels of SK2 do not inhibit DNA synthesis (Okada et al., 2005). SK1-deleted transgenic mice have normal phenotypes, and serum concentrations of S1P are reduced by 50%. However, levels of S1P within a variety of tissues are not different from those of control mice, indicating functional replacement of SK1 by SK2 in normal tissues (Allende et al., 2004). Likewise, genetic ablation of SK2 results in mice with normal fertility and life span, and 25% reduced serum S1P levels (Kharel et al., 2005). Our data (French et al., 2003), and the data of other researchers (Johnson et al., 2005; Van Brocklyn et al., 2005; Kawamori et al., 2006), demonstrate that SK1 is markedly overexpressed in a variety of human cancers, whereas SK2 is typically not (Van Brocklyn et al., 2005), although several types of cancer do have elevated levels of SK2 message (unpublished observations). Therefore, it was unclear whether selective targeting of SK1 or SK2 by SK inhibitors will be sufficient to inhibit tumor growth and induce apoptosis, or whether simultaneous inhibition of SK1 and SK2 will be necessary to prevent the functional redundancy of these isozymes.

Based on this growing body of knowledge implicating SKs in the abnormal growth of cancer cells, we sought to identify novel inhibitors of SK1 and/or SK2 that may serve as effective cancer therapeutics. Screening a chemically diverse small-molecule library by using a recombinant human SK1-fusion protein resulted in the identification of multiple chemotypes (French et al., 2003). Follow-up hit-to-lead efforts resulted in the discovery of ABC294640, an aryladamantane compound with SK inhibitory activity (Smith et al., 2008). The potency of ABC294640 is similar to other SK inhibitors described in the literature (Kono et al., 2001); however, these natural products have unknown selectivities and potential for development. Furthermore, analyses of the kinetics of inhibition of SK2 by ABC294640 clearly indicate that this compound acts as a competitive inhibitor with respect to sphingosine, with a K_i of approximately 10 μM (Fig. 2B). Because the levels of sphingosine in a cell are very low, e.g., compared with ceramide levels (Fig. 3), inhibition of SK2 by ABC294640 is likely to be very efficient. The selective targeting of SK2 was unexpected; however, our studies using small interfering RNAs directed at either SK1 or SK2 demonstrate that ablation of SK2 from tumor cells has greater antiproliferative and antimigratory affects than does depletion of SK1 (P. Gao and C. D. Smith, manuscript in preparation). Because many kinase inhibitors lack specificity, we tested the ability of ABC294640 to inhibit several other kinases. These assays indicated that ABC294640 is highly specific for SK versus protein kinases, making it a viable candidate chemotherapeutic agent.

Our studies on the chemicophysical properties of ABC294640 further support its development. For example, the presence of the pyridine moiety permits protonation of the nitrogen atom and the formation of a hydrochloride salt. This greatly improves the solubility, such that ABC294640·HCl was quite soluble in almost all tested carriers. These broad solubility properties enabled us to test multiple formulations to evaluate their respective in vivo absorption properties. Although all formulations showed encouraging results, we chose 0.375% Polysorbate-80 because of its ease of formation and lower viscosity, which facilitates oral dosing. In addition, long-term stability studies revealed that ABC294640·HCl was highly stable in

0.375% Polysorbate-80 versus the other formulations (data not shown).

Identification of an optimal oral formulation permitted acute and chronic toxicology studies, where we observed excellent toxicity profiles for ABC294640·HCl. A dose of 100 mg/kg, which was determined to be at least 10-fold below than the lowest observed adverse effect level, resulted in ABC294640 plasma levels that exceeded the IC_{50} toward human SK2 and are sufficient for suppression of tumor cell proliferation and migration. Biodistribution studies demonstrated that high concentrations of ABC294640 accumulate in the tumors of intact mice, indicating that the drug does effectively reach its target tissue.

To determine the therapeutic efficacy of the compound, we evaluated ABC294640·HCl in a syngeneic murine breast cancer model and demonstrated significant dose-dependent inhibition of tumor growth. Previous studies have demonstrated that this model is sensitive to SK inhibitors (French et al., 2003). Furthermore, tumor growth inhibition correlated with progressive tumor cell apoptosis and decreases in S1P levels in the tumors compared with vehicle-treated mice. This is the first pharmacodynamic evidence of S1P modulation linked to antitumor activity. We believe that this finding, in conjunction with the low toxicity of ABC294640·HCl, provides validation of SK2 as a chemotherapeutic target.

Studies are currently underway to determine the mechanism of antitumor activity, because SK activity has been linked to survival, inflammatory, and angiogenic pathways. Ideally, SK2 inhibition could lead to modulation of all of these pathways, resulting in tumor inhibition through multiple mechanisms. We also determined that sphingosine levels remained unchanged despite decreases in S1P. This lack of change probably relates to an increase in synthesis of ceramide from sphingosine, resulting in a constant sphingosine level. This would be beneficial in a tumor environment, because increases in ceramide levels cause apoptosis in cancer cells (Kolesnick and Fuks, 2003), and apoptosis does occur in the ABC294640-treated tumor cells. It is noteworthy that we found that SK2 inhibition affects actin structure at time points and concentrations that are nontoxic, suggesting that the compound may also have antimetastatic activity in vivo.

In conclusion, ABC294640·HCl is a first-in-class inhibitor of SK with good pharmacological properties, low toxicity, and anticancer activity. These data support our previous demonstrations that ABC294640·HCl has therapeutic activity in inhibiting diabetes-induced retinal vascular leakage in rats (Maines et al., 2006) and dextran sulfate sodium-induced ulcerative colitis in mice (Maines et al., 2008). Additional unpublished studies also demonstrate that ABC294640·HCl is efficacious in models of Crohn disease, rheumatoid arthritis, and ischemia-reperfusion injury. In all, the data indicate that ABC294640·HCl warrants further developmental efforts to fully determine its potential as an anticancer and anti-inflammatory drug.

References

Allende ML, Sasaki T, Kawai H, Olivera A, Mi Y, van Echten-Deckert G, Hajdu R, Rosenbach M, Keohane CA, Mandala S, et al. (2004) Mice deficient in sphingosine kinase 1 are rendered lymphopenic by FTY720. *J Biol Chem* **279:**52487–52492.

Bielawski J, Szulc ZM, Hannun YA, and Bielawska A (2006) Simultaneous quantitative analysis of bioactive sphingolipids by high-performance liquid chromatography-tandem mass spectrometry. *Methods* **39:**82–91.

Cuvillier O (2007) Sphingosine kinase-1—a potential therapeutic target in cancer. *Anticancer Drugs* **18:**105–110.

Cuvillier O, Pirianov G, Kleuser B, Vanek PG, Coso OA, Gutkind S, and Spiegel S (1996) Suppression of ceramide-mediated programmed cell death by sphingosine-1-phosphate. *Nature* **381:**800–803.

Döll F, Pfeilschifter J, and Huwiler A (2005) The epidermal growth factor stimulates sphingosine kinase-1 expression and activity in the human mammary carcinoma cell line MCF7. *Biochim Biophys Acta* **1738:**72–81.

Edsall LC, Cuvillier O, Twitty S, Spiegel S, and Milstien S (2001) Sphingosine kinase expression regulates apoptosis and caspase activation in PC12 cells. *J Neurochem* **76:**1573–1584.

French KJ, Schrecengost RS, Lee BD, Zhuang Y, Smith SN, Eberly JL, Yun JK, and Smith CD (2003) Discovery and evaluation of inhibitors of human sphingosine kinase. *Cancer Res* **63:**5962–5969.

French KJ, Upson JJ, Keller SN, Zhuang Y, Yun JK, and Smith CD (2006) Antitumor activity of sphingosine kinase inhibitors. *J Pharmacol Exp Ther* **318:**596–603.

Gamble JR, Xia P, Hahn CN, Drew JJ, Drogemuller CJ, Brown D, and Vadas MA (2006) Phenoxodiol, an experimental anticancer drug, shows potent antiangiogenic properties in addition to its antitumour effects. *Int J Cancer* **118:**2412–2420.

Hait NC, Oskeritzian CA, Paugh SW, Milstien S, and Spiegel S (2006) Sphingosine kinases, sphingosine 1-phosphate, apoptosis and diseases. *Biochim Biophys Acta* **1758:**2016–2026.

Hait NC, Sarkar S, Le Stunff H, Mikami A, Maceyka M, Milstien S, and Spiegel S (2005) Role of sphingosine kinase 2 in cell migration toward epidermal growth factor. *J Biol Chem* **280:**29462–29469.

Huwiler A and Zangemeister-Wittke U (2007) Targeting the conversion of ceramide to sphingosine 1-phosphate as a novel strategy for cancer therapy. *Crit Rev Oncol Hematol* **63:**150–159.

Igarashi Y, Hakomori S, Toyokuni T, Dean B, Fujita S, Sugimoto M, Ogawa T, el-Ghendy K, and Racker E (1989) Effect of chemically well-defined sphingosine and its *N*-methyl derivatives on protein kinase C and src kinase activities. *Biochemistry* **28:**6796–6800.

Johnson KR, Johnson KY, Crellin HG, Ogretmen B, Boylan AM, Harley RA, and Obeid LM (2005) Immunohistochemical distribution of sphingosine kinase 1 in normal and tumor lung tissue. *J Histochem Cytochem* **53:**1159–1166.

Kawamori T, Osta W, Johnson KR, Pettus BJ, Bielawski J, Tanaka T, Wargovich MJ, Reddy BS, Hannun YA, Obeid LM, et al. (2006) Sphingosine kinase 1 is up-regulated in colon carcinogenesis. *FASEB J* **20:**386–388.

Kharel Y, Lee S, Snyder AH, Sheasley-O'Neill SL, Morris MA, Setiady Y, Zhu R, Zigler MA, Burcin TL, Ley K, et al. (2005) Sphingosine kinase 2 is required for modulation of lymphocyte traffic by FTY720. *J Biol Chem* **280:**36865–36872.

King CC, Zenke FT, Dawson PE, Dutil EM, Newton AC, Hemmings BA, and Bokoch GM (2000) Sphingosine is a novel activator of 3-phosphoinositide-dependent kinase 1. *J Biol Chem* **275:**18108–18113.

Kohama T, Olivera A, Edsall L, Nagiec MM, Dickson R, and Spiegel S (1998) Molecular cloning and functional characterization of murine sphingosine kinase. *J Biol Chem* **273:**23722–23728.

Kolesnick R and Fuks Z (2003) Radiation and ceramide-induced apoptosis. *Oncogene* **22:**5897–5906.

Kono K, Tanaka M, Ono Y, Hosoya T, Ogita T, and Kohama T (2001) S-15183a and b, new sphingosine kinase inhibitors, produced by a fungus. *J Antibiot (Tokyo)* **54:**415–420.

Le Scolan E, Pchejetski D, Banno Y, Denis N, Mayeux P, Vainchenker W, Levade T, and Moreau-Gachelin F (2005) Overexpression of sphingosine kinase 1 is an oncogenic event in erythroleukemic progression. *Blood* **106:**1808–1816.

Lee BD, French KJ, Zhuang Y, and Smith CD (2003) Development of a syngeneic in vivo tumor model and its use in evaluating a novel P-glycoprotein modulator, PGP-4008. *Oncol Res* **14:**49–60.

Lee OH, Kim YM, Lee YM, Moon EJ, Lee DJ, Kim JH, Kim KW, and Kwon YG (1999) Sphingosine 1-phosphate induces angiogenesis: its angiogenic action and signaling mechanism in human umbilical vein endothelial cells. *Biochem Biophys Res Commun* **264:**743–750.

Liu H, Sugiura M, Nava VE, Edsall LC, Kono K, Poulton S, Milstien S, Kohama T, and Spiegel S (2000) Molecular cloning and functional characterization of a novel mammalian sphingosine kinase type 2 isoform. *J Biol Chem* **275:**19513–19520.

Maceyka M, Sankala H, Hait NC, Le Stunff H, Liu H, Toman R, Collier C, Zhang M, Satin LS, Merrill AH Jr, et al. (2005) SphK1 and SphK2, sphingosine kinase isoenzymes with opposing functions in sphingolipid metabolism. *J Biol Chem* **280:**37118–37129.

Maines LW, Fitzpatrick LR, French KJ, Zhuang Y, Xia Z, Keller SN, Upson JJ, and Smith CD (2008) Suppression of ulcerative colitis in mice by orally available inhibitors of sphingosine kinase. *Dig Dis Sci* **53:**997–1012.

Maines LW, French KJ, Wolpert EB, Antonetti DA, and Smith CD (2006) Pharmacologic manipulation of sphingosine kinase in retinal endothelial cells: implications for angiogenic ocular diseases. *Invest Ophthalmol Vis Sci* **47:**5022–5031.

McDonald OB, Hannun YA, Reynolds CH, and Sahyoun N (1991) Activation of casein kinase II by sphingosine. *J Biol Chem* **266:**21773–21776.

Nakade Y, Banno Y, T-Koizumi K, Hagiwara K, Sobue S, Koda M, Suzuki M, Kojima T, Takagi A, Asano H, et al. (2003) Regulation of sphingosine kinase 1 gene expression by protein kinase C in a human leukemia cell line, MEG-O1. *Biochim Biophys Acta* **1635:**104–116.

Nava VE, Hobson JP, Murthy S, Milstien S, and Spiegel S (2002) Sphingosine kinase type 1 promotes estrogen-dependent tumorigenesis of breast cancer MCF-7 cells. *Exp Cell Res* **281:**115–127.

Ogretmen B (2006) Sphingolipids in cancer: regulation of pathogenesis and therapy. *FEBS Lett* **580:**5467–5476.

Okada T, Ding G, Sonoda H, Kajimoto T, Haga Y, Khosrowbeygi A, Gao S, Miwa N, Jahangeer S, and Nakamura S (2005) Involvement of N-terminal-extended form of sphingosine kinase 2 in serum-dependent regulation of cell proliferation and apoptosis. *J Biol Chem* **280:**36318–36325.

Pchejetski D, Golzio M, Bonhoure E, Calvet C, Doumerc N, Garcia V, Mazerolles C, Rischmann P, Teissié J, Malavaud B, et al. (2005) Sphingosine kinase-1 as a chemotherapy sensor in prostate adenocarcinoma cell and mouse models. *Cancer Res* **65:**11667–11675.

Sarkar S, Maceyka M, Hait NC, Paugh SW, Sankala H, Milstien S, and Spiegel S (2005) Sphingosine kinase 1 is required for migration, proliferation and survival of MCF-7 human breast cancer cells. *FEBS Lett* **579:**5313–5317.

Shu X, Wu W, Mosteller RD, and Broek D (2002) Sphingosine kinase mediates vascular endothelial growth factor-induced activation of ras and mitogen-activated protein kinases. *Mol Cell Biol* **22:**7758–7768.

Smith CD, French KJ, and Zhuang Y (2008) inventors; Apogee Biotechnology Corporation, assignee. Sphingosine kinase inhibitors. U.S. Patent 7,338,961. 2008 Mar 4.

Sukocheva OA, Wang L, Albanese N, Pitson SM, Vadas MA, and Xia P (2003) Sphingosine kinase transmits estrogen signaling in human breast cancer cells. *Mol Endocrinol* **17:**2002–2012.

Van Brocklyn JR, Jackson CA, Pearl DK, Kotur MS, Snyder PJ, and Prior TW (2005) Sphingosine kinase-1 expression correlates with poor survival of patients with glioblastoma multiforme: roles of sphingosine kinase isoforms in growth of glioblastoma cell lines. *J Neuropathol Exp Neurol* **64:**695–705.

Vann LR, Payne SG, Edsall LC, Twitty S, Spiegel S, and Milstien S (2002) Involvement of sphingosine kinase in TNF-alpha-stimulated tetrahydrobiopterin biosynthesis in C6 glioma cells. *J Biol Chem* **277:**12649–12656.

Xia P, Gamble JR, Wang L, Pitson SM, Moretti PA, Wattenberg BW, D'Andrea RJ, and Vadas MA (2000) An oncogenic role of sphingosine kinase. *Curr Biol* **10:**1527–1530.

Address correspondence to: Dr. Charles D. Smith, Apogee Biotechnology Corporation, 1214 Research Blvd, Suite 1016, Hummelstown, PA 17036. E-mail: cdsmith@apogee-biotech.com